The *Pseudomonas* Quorum-Sensing Regulator RsaL Belongs to the Tetrahelical Superclass of H-T-H Proteins[▽]

Giordano Rampioni,[1] Fabio Polticelli,[1] Iris Bertani,[2] Karima Righetti,[1] Vittorio Venturi,[2] Elisabetta Zennaro,[1] and Livia Leoni[1]*

Department of Biology, University Roma Tre, Viale Marconi, 446, 00146, Rome, Italy,[1] and International Centre for Genetic Engineering and Biotechnology, Padriciano, 99, 34012, Trieste, Italy[2]

In the opportunistic human pathogen *Pseudomonas aeruginosa*, quorum sensing (QS) is crucial for virulence. The RsaL protein directly represses the transcription of *lasI*, the synthase gene of the main QS signal molecule. On the basis of sequence homology, RsaL cannot be predicted to belong to any class of characterized DNA-binding proteins. In this study, an in silico model of the RsaL structure was inferred showing that RsaL belongs to the tetrahelical superclass of helix-turn-helix proteins. The overall structure of RsaL is very similar to the *N*-terminal domain of the lambda *c*I repressor and to the POU-specific domain of the mammalian transcription factor Oct-1 (Oct-1 POUs). Moreover, residues of Oct-1 POUs important for structural stability and/or DNA binding are conserved in the same positions in RsaL and in its homologs found in GenBank. These residues were independently replaced with Ala, and the activities of the mutated variants of RsaL were compared to that of the wild-type counterpart in vivo by complementation assays and in vitro by electrophoretic mobility shift assays. The results validated the RsaL in silico model and showed that residues Arg 20, Gln 38, Ser 42, Arg 43, and Glu 45 are important for RsaL function. Our data indicate that RsaL could be the founding member of a new protein family within the tetrahelical superclass of helix-turn-helix proteins. Finally, the minimum DNA sequence required for RsaL binding on the *lasI* promoter was determined, and our data support the hypothesis that RsaL binds DNA as a dimer.

Quorum sensing (QS) is a widespread bacterial communication system based on the production of signal molecules. In a bacterial population, when the concentration of the signal molecule reaches a threshold corresponding to a certain cell density, individual cells of the population coordinately respond by reprogramming the expression levels of several genes (16).

Pseudomonas aeruginosa is an important opportunistic human pathogen able to establish severe and hard-to-eradicate infections in immunocompromised hosts, such as burned, AIDS, and cystic fibrosis patients. In the last case, a persistent *P. aeruginosa* lung infection is the major cause of death (14). QS plays a key role in the *P. aeruginosa* infection process because it regulates the production of many virulence factors, as well as biofilm formation (24). Moreover, the QS signal molecules themselves play important roles in the cross talk between host and parasite (27). In animal models, *P. aeruginosa* mutants impaired in QS display reduced virulence, and QS-inhibitory compounds are effective in clearing the infecting bacteria and in reducing mortality (9, 19).

The QS response in *P. aeruginosa* is controlled by many regulators that are involved in the modulation of signal molecule production. The structures and modes of action of these regulators and their real impacts on the production of the QS signal molecules, as well as the stimuli to which they respond, in most cases are unknown (21, 26).

The RsaL protein is a pivotal negative regulator of QS, since

the production of the main QS signal molecule of *P. aeruginosa*, i.e., *N*-3-oxo-dodecanoyl homoserine lactone (3OC12-HSL), is dramatically enhanced in an *rsaL* mutant strain. RsaL directly represses *lasI*, the 3OC12-HSL synthase gene, by binding its promoter, P*lasI* (7, 18). Importantly, besides the 3OC12-HSL-dependent activator LasR, RsaL is the only QS regulator known to bind P*lasI* (21, 22). The demonstration that RsaL is a DNA-binding protein has been of particular interest, considering that it shows homology only with the orthologous RsaL proteins of *Pseudomonas putida* strains IsoF, WCS358, and PCL1445 and with putative proteins present in some of the sequenced microbial genomes, whose functions have not yet been determined or predicted (3, 8, 18, 25). In addition, conventional in silico methods for the identification of domain-specific signature patterns (CDD [http://www.ncbi.nlm.nih.gov/Structure/cdd/cdd.shtml] and SMART [http://smart.embl-heidelberg.de]) did not highlight any known domain for DNA binding in RsaL, suggesting that the protein could belong to a new class of transcriptional regulators.

In this study, an in silico model of RsaL structure has been inferred and experimentally validated, showing that RsaL belongs to the tetrahelical superclass of helix-turn-helix (H-T-H)-containing proteins (1). Many transcriptional factors from the three superkingdoms of life contain H-T-H domains belonging to this wide structural class, such as the *N*-terminal domain of the lambda *c*I repressor (λ*c*I-NTD) and the POU-specific domain of the mammalian transcription factor Oct-1 (Oct-1 POUs). The POU domain is the DNA-binding domain of an important class of eukaryotic transcription factors involved in developmental regulation and cellular housekeeping. It is a bipartite structure composed of two autonomous DNA-bind-

---

TABLE 1. Oligonucleotides utilized for site-directed mutagenesis of RsaL[PAO]

Name	Sequence (5′–3′)[a]	Position[b]	Introduced mutation
FW-RsaL	ATGCCATGGCTTCACACGAGAGAA	+1	
RV-RsaL	CCCAAGCTTCTCTCTGATCTTGCCTCT	+240	
FW R20A	AAGGCCACCGCCACCGCCC	+49	R20A: CGC→GCC
RV-R20A	GGGCGGTGGCGGTGGCCTT	+67	R20A: CGC→GCC
FW-Q38A	GGGATAAGCGCCTCCTGCGGC	+103	Q38A: CAA→GCC
RV-Q38A	GCCGCAGGAGGCGCTTATCCC	+123	Q38A: TTG→GGC
FW-C40A	GCCAATCCGCCGGCAGTCGT	+110	C40A: TGC→GCC
RV-C40A	ACGACTGCCGGCGGATTGGC	+129	C40A: GCA→GGC
FW-S42A	TCCTGCGGCGCCCGTTTCGAG	+115	S42A: AGT→GCC
RV-S42A	CTCGAAACGGGCGCCGCAGGA	+135	S42A: ACT→GGC
FW-R43A	CTGCGGCAGTGCCTTCGAGAATG	+117	R43A: CGT→GCC
RV-R43A	CATTCTCGAAGGCACTGCCGCAG	+139	R43A: ACG→GGC
FW-E45A	CAGTCGTTTCGCGAATGGCGAG	+123	E45A: GAG→GCG
RV-E45A	CTCGCCATTCGCGCAACGACTG	+144	E45A: CTC→CGC
FW-R20E	AAGGCCACCGAGACCGCCCG	+49	R20E: CGC→GAG
RV-R20E	CGGGCGGTCTCGGTGGCCTT	+68	R20E: GCG→CTC
FW-E45R	CAGTCGTTTCCGCAATGGCGAGA	+123	E45R: GAG→CGC
RV-E45R	TCTCGCCATTGCGGAAACGACTG	+145	E45R: CTC→GCG
P0FW	GGGTACCAATAATTTTGTTTAACTTTA	329	
P0RV	GGGGATCCATTGCTCAGCGGTGGCAGC	71	

[a] Introduced restriction sites (NcoI, HindIII, KpnI, and BamHI) are underlined. Substituted nucleotides are in boldface.
[b] Distance in base pairs from the *rsaL* ATG (for P0FW and P0RV, the position with respect to the pET28b(+) sequence is given).

ing subdomains, the POU-specific domain and the POU homeodomain, that are covalently connected by a flexible peptide linker (17). Interestingly, we have found that residues of the Oct-1 POUs important for structural stability and/or DNA binding are conserved in the same positions in RsaL and its homologs.

The characterization of the minimum consensus sequence for RsaL binding to P*lasI* and data suggesting that the protein binds DNA as a homodimer are also reported.

MATERIALS AND METHODS

In silico modeling. The three-dimensional structures of RsaL from *P. aeruginosa* PAO1 (7) and from *P. putida* WCS358 (3) were modeled using the molecular-modeling software Rosetta (4) as implemented on the Robetta web server (http://robetta.bakerlab.org/).

Recombinant DNA techniques. Preparation of plasmid DNA, purification of DNA fragments, ligation, and transformation of *Escherichia coli* were carried out by using standard procedures (20). PCR amplifications were performed using Red-*Taq* polymerase (Sigma). The sequences of oligonucleotides used for PCR are shown in Table 1. Automated sequencing was performed to check the DNA inserts of all the plasmids constructed in this study (MWG Biotech).

Site-directed mutagenesis and protein purification. Site-directed mutations were generated in *rsaL* using the splicing by overlap extension PCR method (10) with the primers described in Table 1. In the first step, two distinct PCRs (PCR-1 and PCR-2) were carried out for each *rsaL* derivative mutant, using chromosomal *P. aeruginosa* DNA as a template. Each PCR-1 was performed with the forward (FW) primer FW-RsaL and with a mutagenic reverse (RV) primer carrying the mutation in the desired codon. Each PCR-2 was performed with a mutagenic FW primer complementary to the RV primer utilized in the corresponding PCR-1 and with primer RV-RsaL. In the second PCR step, products obtained from PCR-1 and PCR-2 for each mutation were spliced together using the FW-RsaL and RV-RsaL primers. To generate *rsaL*[R20E-E45R], a first round of two-step PCR mutagenesis was performed to introduce the Arg 20 Glu substitution in the RsaL coding sequence. Afterwards, the PCR product of this first round was used as a template for a second round of two-step PCR mutagenesis, in order to introduce the second mutation, Glu 45 Arg.

The different PCR products were digested by NcoI and HindIII, ligated into the expression vector pET28b(+) (Novagen), and introduced into the expression host *E. coli* BL21(DE3)pLysS (Novagen) for overexpression. Purification by Ni²⁺ affinity of mutant proteins, expressed by the different pET28b(+) derivatives and six-His tagged at the C terminus, was carried out as previously described for RsaL[PAO] (18). Proteins were further purified by gel permeation

chromatography on a Superdex 200 HR column (Amersham Pharmacia Biotech).

Complementation assay and measurement of 3OC12-HSL. In order to express the wild-type and mutated *rsaL* variants fused to six-His coding sequences in *P. aeruginosa* PAO1 (wild type; University of Washington Genome Center) and in its *rsaL* derivative (University of Washington Genome Center), the differently mutated variants of *rsaL* were cloned into the broad-host-range expression vector pBBR1MCS-5 under the control of the constitutive P*lac* promoter (13). For this purpose, the different pET28b(+) derivatives constructed to purify the wild-type and mutated RsaL proteins (see above) were used as DNA templates for PCR, together with primers P0FW and P0RV (Table 1). The different PCR products were digested by KpnI and BamHI, ligated into pBBR1MCS-5, and conjugated into *P. aeruginosa* PAO1 and its *rsaL*-mutated derivative as previously described (18). 3OC12-HSL was extracted from spent-growth medium and quantified by the use of a *P. putida* SM17(prsaL220) HSL biosensor strain. The *P. putida* SM17(prsaL220) sensor strain was constructed based on the PpuI/R quorum-sensing system of *P. putida* WCS358, which produces and responds to the 3OC12-HSL signal molecule (3). In this strain, 3OC12-HSL is produced by the PpuI synthase, encoded by the *ppuI* gene that is contiguous to *rsaL* (3). The 3OC12-HSL response regulator PpuR activates transcription of both *ppuI* and *rsaL* (3). A kanamycin resistance cassette was inserted within a BamHI-KpnI fragment between the SalI-XhoI sites of *ppuI* and *rsaL*, respectively, yielding pMPQS::Km. This plasmid was then used to inactivate the chromosomal *ppuI* and *rsaL* genes of *P. putida* by a marker exchange technique. Plasmid pPH1JI was used as the incoming IncP1-incompatible plasmid (6). The resultant *P. putida* SM17 strain contained a deletion in both *ppuI* and *rsaL* and consequently did not produce 3OC12-HSL and the RsaL repressor. 3OC12-HSL could then be quantified by measuring β-galactosidase activity using *P. putida* SM17 carrying plasmid prsaL220. This plasmid contains the PpuR–3OC12-HSL-regulated *rsaL* promoter transcriptionally fused to *lacZ* (3).

N-Acyl-homoserine lactone extracts of different *P. aeruginosa* strains were prepared as previously described (18), and the quantity of 3OC12-HSL was determined using *P. putida* SM17(prsal220). Overnight cultures of *P. putida* SM17(prsaL220) were diluted in LB medium to an A_{660} of 0.1. The *N*-acyl-homoserine lactone extract was then added, and after 6 h of growth at 30°C, β-galactosidase activity was determined (15). The amounts for a minimal and for a maximal saturated response were determined using synthetic 3OC12-HSL, and the quantifications corresponded in the linear dose response between these two values. This sensor is very specific for detection and quantification of 3OC12-HSL, as several synthetic *N*-acyl-homoserine lactones were tested, and apart from the cognate signal molecule, only 3OC10-HSL was an agonist (data not shown). The linear dose responses for 3OC12-HSL were from 0.1 μM to 5 μM, making this a well-suited biosensor for quantification of this molecule.
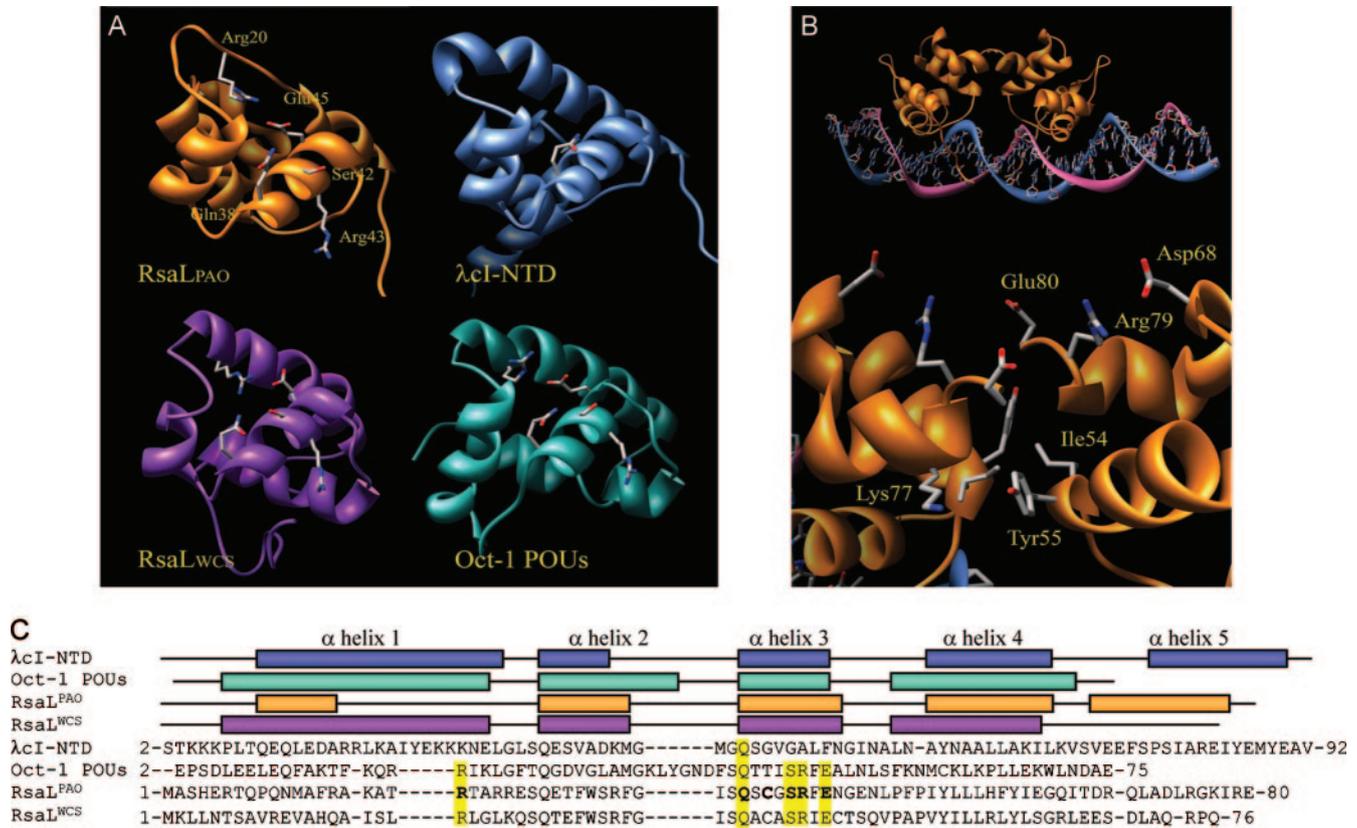
FIG. 1. In silico model of RsaL. (A) Schematic representation of the molecular models of RsaL^{PAO} and RsaL^{WCS} and of the experimentally determined structures of λcI-NTD (11) (protein data base [PDB] code, 1RIO) and Oct-1 POUs (5) (PDB code, 1CQT). Selected residues are shown in stick representation and labeled in the RsaL^{PAO} structure. Corresponding residues in the other three proteins are also shown. (B) Global and enlarged views of the complex between the putative RsaL^{PAO} dimer and DNA, modeled on the basis of the λcI-NTD–DNA complex. Residues involved in the interactions between the two monomers are shown in stick representation and are labeled on only one of the two monomers. (C) Structure-based sequence alignment of RsaL^{PAO}, RsaL^{WCS}, λcI-NTD, and Oct-1 POUs. The secondary structure of each protein is shown above the alignment. Residues shown in stick representation in panel A are highlighted in yellow. Residues selected for site-directed mutagenesis are in boldface.

EMSA. Different DNA probes were obtained by annealing in vitro complementary oligonucleotides corresponding either to nucleotides −4 to −28 of the wild-type *lasI* promoter (the numbering refers to the *lasI* transcription start point [23]) or to the same sequence carrying substitutions (see Fig. 5A). The annealed oligonucleotides were cloned into pDRIVE (QIAGEN), excised by EcoRI digestion, and 5′ end labeled. The procedures for [α-^{32}P]dATP labeling of the probes, as well as the electrophoretic mobility shift assay (EMSA), have been previously described (18). The concentrations either of the different proteins (see the EMSA experiment shown in Fig. 3) or of the different DNA probes (see the EMSA experiment shown in Fig. 5) were previously equilibrated, and the experiments were carried out simultaneously, with identical polyacrylamide gels run in parallel.

RESULTS

RsaL is predicted to belong to the tetrahelical superclass of H-T-H proteins. The orthologous RsaL proteins of *P. aeruginosa* PAO1 and *P. putida* WCS358 (RsaL^{PAO} and RsaL^{WCS}, respectively) are 42% identical. Their three-dimensional structures were independently modeled using the Rosetta software (4), which selected the structures of λcI-NTD (11) and of Oct-1 POUs (5) as templates for comparative modeling for RsaL^{PAO} and RsaL^{WCS}, respectively (Fig. 1A). Despite the lack of sequence homology, λcI-NTD and Oct-1 POUs share a common fold consisting of four alpha helices, in which helices 2 and 3

form an H-T-H motif for DNA binding, with helix 3 directly contacting the DNA major groove (2, 5, 11, 12). This bundle characterizes the tetrahelical H-T-H superclass, one of the major monophyletic groups in which the H-T-H proteins are clustered (1). Both RsaL models display this four-helix H-T-H fold, while differences are observed in the N- and C-terminal regions between the two models. In addition, despite the low overall sequence homology between Oct-1 POUs, RsaL^{PAO}, and RsaL^{WCS}, a striking conservation of several residues (Gln 38, Ser 42, Arg 43, and Glu 45; the numbering refers to RsaL^{PAO}) is observed in the region corresponding to helix 3 (residues 38 to 46). Also, Arg 20 in helix 1, Glu 27 at the beginning of helix 2, and Ser 37 just before the beginning of helix 3 are conserved. With the exception of Gln 27 and Gln 38, the above-mentioned residues are not conserved in λcI-NTD (Fig. 1C). It has been determined that Gln 38, Ser 42, and Arg 43 are important for the specific interaction of Oct-1 POUs with its target DNA (5). We also observed in DNase I protection experiments that the ATGC DNA motif typically bound by Oct-1 POUs is present within the DNA region protected by RsaL^{PAO} (5, 17, 18).

Another interesting feature that is predicted to be shared

by Oct-1 POUs, RsaL^{PAO}, and RsaL^{WCS} is the presence of a salt bridge between Arg 20 and Glu 45 (Fig. 1A). In λcI-NTD, this salt bridge is lacking, while in Oct-1 POUs, it links helices 1 and 3, contributing to the overall stability of the protein (5).

Validation of the model: key functional residues are conserved in RsaL^{PAO} and Oct-1 POUs. In order to experimentally confirm the proposed structural model for RsaL^{PAO}, conserved residues predicted to contact DNA (Gln 38, Ser 42, and Arg 43) and to form the salt bridge (Arg 20 and Glu 45) were mutated to Ala. As a control, the nonconserved Cys 40 residue that, although located in helix 3, is not predicted to interact with DNA in our model was also replaced with Ala. In addition, the residues predicted to form the salt bridge were inverted by introducing the double substitution Arg 20 Glu/Glu 45 Arg.

A recent study showed that 3OC12-HSL production was enhanced in an *rsaL* mutant of *P. aeruginosa* PAO1 (18). This unambiguous phenotype makes it possible to compare in vivo the activities of the wild-type and mutated variants of RsaL^{PAO} by a complementation assay. Therefore, the *rsaL* wild-type and mutated coding sequences, fused with a six-His tag at their C termini to allow the detection of the expressed proteins by Western assay, were cloned into the broad-host-range expression plasmid pBBR1MCS-5 and independently introduced into the *rsaL* mutant of *P. aeruginosa* PAO1. 3OC12-HSLs were extracted from the growth media of the strains carrying the different plasmids, and their levels were compared using the *P. putida* SM17(prsaL220) sensor strain that was constructed here for the purpose (see Materials and Methods). Briefly, in this strain, the expression of *lacZ* is under the control of a 3OC12-HSL-responsive promoter, so that β-galactosidase activity is proportional to the amount of 3OC12-HSL present in the growth medium. The results of this experiment (Fig. 2A) showed that the 3OC12-HSL level produced by the *P. aeruginosa* wild type was enhanced about fivefold in the *P. aeruginosa rsaL* mutant. Complementation of this mutant with *rsaL* or with its mutated variants *rsaL*^{C40A} and *rsaL*$^{R20E-E45R}$ restored the 3OC12-HSL production to wild-type levels. Conversely, 3OC12-HSL levels were not restored upon complementation of the *rsaL* mutant strain with plasmids expressing the mutated proteins RsaL^{R20A}, RsaL^{Q38A}, RsaL^{S42A}, RsaL^{R43A}, and RsaL^{E45A} (Fig. 2A). The Western analysis carried out on the soluble cellular fractions of the same cultures in which 3OC12-HSL was measured showed that the levels of wild-type RsaL^{PAO} and its mutated derivatives were comparable, demonstrating that the lack of complementation ability was not due to decreased expression of the recombinant proteins (Fig. 2B). Therefore, RsaL^{PAO} residues Arg 20, Gln 38, Ser 42, Arg 43, and Glu 45 are essential for the activity of RsaL^{PAO} in the cell.

At the molecular level, RsaL^{PAO} acts as a transcriptional repressor of the 3OC12-HSL synthase gene by direct binding to its promoter, P*lasI* (18). In order to assess whether the introduced mutations affect the DNA-binding activity of RsaL^{PAO}, we performed EMSAs comparing the ability of purified wild-type RsaL^{PAO} to bind a DNA probe encompassing the RsaL^{PAO}-binding site of P*lasI* with those of its mutated derivatives. All of the proteins were purified to homogeneity, and their concentrations were equilibrated (Fig. 3A). Incubation of the DNA probe with wild-type RsaL^{PAO} led to the formation of a
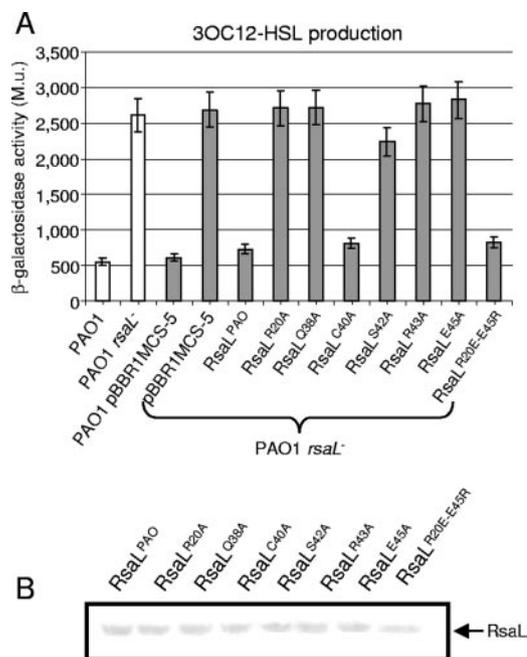

FIG. 2. In vivo validation of the RsaL^{PAO} model. (A) Measurement of 3OC12-HSL produced by *P. aeruginosa* PAO1 and its *rsaL* mutant derivative (white bars) and by the same strains carrying either the pBBR1-MCS5 plasmid, as a control, or its derivatives expressing RsaL^{PAO} or the indicated mutant proteins (gray bars). 3OC12-HSL was extracted from the spent-growth medium of each strain and quantitatively measured as described in Materials and Methods, using the *P. putida* SM17(prsaL220) strain, in which β-galactosidase activity (given in Miller units [M.u.]) is proportional to the levels of 3OC12-HSL. Standard deviations (error bars) are based on the mean values for three parallel cultures. (B) Western hybridization performed with anti-six-His tag antibody (Sigma) on the cellular soluble fractions derived from the same cultures in which 3OC12-HSL production was measured. The protein expressed in each sample is indicated above its lane.

complex having lower electrophoretic mobility than the probe alone (Fig. 3B). This result was expected and was consistent with that of a previously published EMSA experiment (18). RsaL^{PAO} was able to shift about 50% of the probe at a concentration of 10 nM, while RsaL^{Q38A}, RsaL^{S42A}, and RsaL^{R43A} were unable to shift the same DNA probe even at a concentration 625-fold higher (Fig. 3B; only EMSA carried out with RsaL^{Q38A} is shown). On the other hand, the DNA-binding ability of RsaL^{C40A} was comparable to that of the wild-type protein (Fig. 3B). Moreover, the substitution Arg 20 Ala or Glu 45 Ala had a strong negative influence on the RsaL DNA-binding ability that was partially restored by inverting the positions of these residues in RsaL$^{R20E-E45R}$ (Fig. 3B). The above-mentioned results validated our proposed in silico model, in which the helix 3 residues Gln 38, Ser 42, and Arg 43, but not Cys 40, are important to establish direct interactions with DNA, while Arg 20 and Glu 45 stabilize the RsaL^{PAO} structure by forming a salt bridge.

RsaL^{PAO} binds to an eptameric inverted repeat as a dimer. The RsaL^{PAO}-binding site on P*lasI* was previously characterized by DNase I protection experiments and contains two inverted repeats forming a palindrome, suggesting that RsaL^{PAO} binds DNA as a dimer (18). Accordingly, the modeling of the
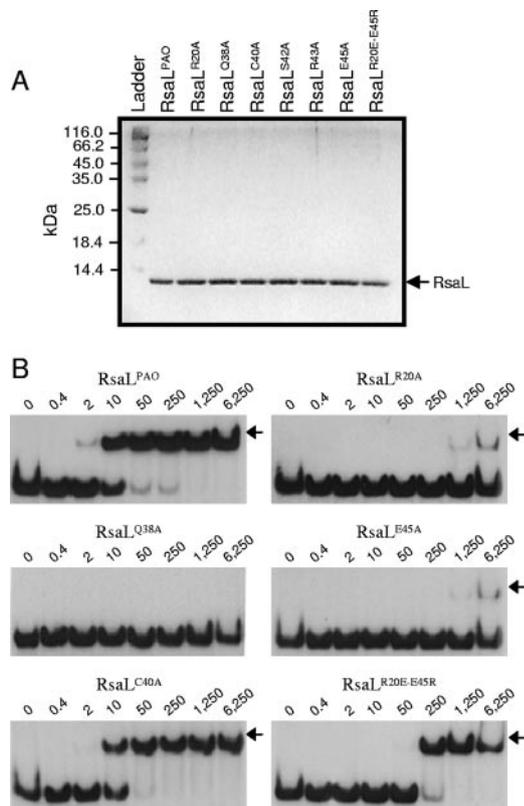
FIG. 3. In vitro validation of the RsaL[PAO] model. (A) Sodium dodecyl sulfate-polyacrylamide gel electrophoresis showing that purified RsaL[PAO] and its mutated derivatives (indicated above each lane) are very pure and that their concentrations are equilibrated. Two microliters of each protein was loaded on the gel. Ladder, PageRuler protein ladder (Fermentas); the molecular mass of each band is indicated on the left. (B) EMSA carried out with a DNA probe encompassing the RsaL[PAO]-binding site on P*lasI* and either RsaL[PAO] or its mutated derivatives (indicated above each gel). The EMSAs were carried out simultaneously, starting from the same mixture containing the DNA probe, with identical polyacrylamide gels run in parallel. RsaL[S42A] and RsaL[R43A] showed an EMSA pattern (not shown) identical to that of RsaL[Q38A]. The RsaL-DNA complexes are indicated by arrows. The protein concentration (nM) for each sample is indicated above its lane.

FIG. 4. Hill plot inferred from the EMSA performed with RsaL[PAO] and a DNA probe encompassing the RsaL[PAO]-binding site on the *lasI* promoter (shown in Fig. 3B). The amounts of bound and free probe for each lane were measured by a densitometric analysis carried out with the software Kodak 1D 3.5. The protein concentration is in molar excess with respect to the probe concentration. The Hill coefficient ($n_{50} = 1.4$) indicates cooperative binding.

RsaL[PAO] dimer, based on the λ*c*I-NTD dimer, revealed the presence of several interactions that could stabilize the formation of the RsaL[PAO] dimer (Fig. 1B). In particular, Lys 77 on one monomer could form a favorable electrostatic interaction with Tyr 55 on the other monomer, and Asp 68, Arg 79, and Glu 80 could form an extended charge network with the corresponding residues of the second monomer. In addition, hydrophobic interactions could take place between Ile 54 and Tyr 55 of both monomers, potentially providing additional stability to the dimer.

To assess the oligomeric state of RsaL[PAO], we performed gel permeation chromatography showing that RsaL is a monomer in solution (data not shown). However, the Hill plot inferred from the EMSA performed with RsaL[PAO] indicated that binding of this protein to the target DNA is cooperative (Hill coefficient, 1.4) (Fig. 4), suggesting that DNA could play a role in RsaL dimerization. Moreover, the absence of intermediate complexes in the EMSA indicates that only the com-
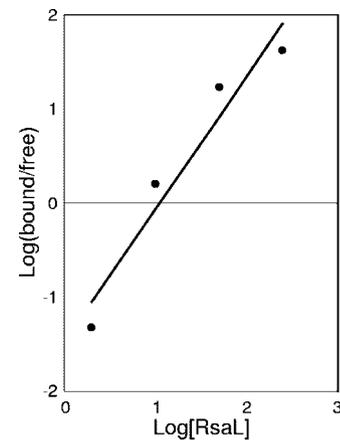
plex between an RsaL[PAO] dimer and DNA could be stable enough to be detectable. If this is the case, disrupting the palindromic structure of the DNA probe bound by RsaL[PAO] would lead to the abolition of the complex formation in an EMSA assay. To validate this hypothesis, we performed EMSA experiments using mutated DNA probes in which the palindromic structure of the RsaL[PAO]-binding site was disrupted. To select the nucleotides to be mutagenized, we considered that Oct-1 POUs specifically contact the ATGC motif, mainly through the conserved residues Gln 38, Ser 42, and Arg 43 (5, 12). This DNA motif is also present in the core of the right repeat of the RsaL[PAO]-binding site (complementary strand) and is partially conserved in the left repeat (Fig. 5A). Thus, we constructed two DNA probes in which the ATG sequence of the left repeat or the ATGC sequence of the right repeat were alternatively substituted (Fig. 5A, probes I and II, respectively), and the abilities of RsaL[PAO] to bind the mutated and wild-type DNA fragments were compared by EMSA. The results showed that the substitution of each of these sequences abrogated RsaL[PAO] binding even at protein concentrations 625-fold higher than that sufficient to completely shift the same amount of wild-type probe. These results strongly support our hypothesis that the formation of a dimer of RsaL[PAO] on the target DNA is necessary for the formation of a stable complex (Fig. 5B; EMSA carried out with probe II, identical to that with probe I, is not shown).

To better define the minimum sequence requirements for RsaL[PAO] binding to P*lasI*, we tested the abilities of a set of DNA probes (mutated in each pair of specular nucleotides contributing to form the palindrome) to bind RsaL[PAO] (Fig. 5A, probes III to XI). We found that the EMSA carried out with probes III to V had a pattern identical to that obtained with the wild-type probe, indicating that the mutagenized nucleotides are not involved in the formation of the RsaL[PAO]-DNA complex (In Fig. 5B, only the EMSA with the wild-type probe is shown). On the other hand, the DNA probes VI to VIII had a pattern identical to that of probe I and therefore
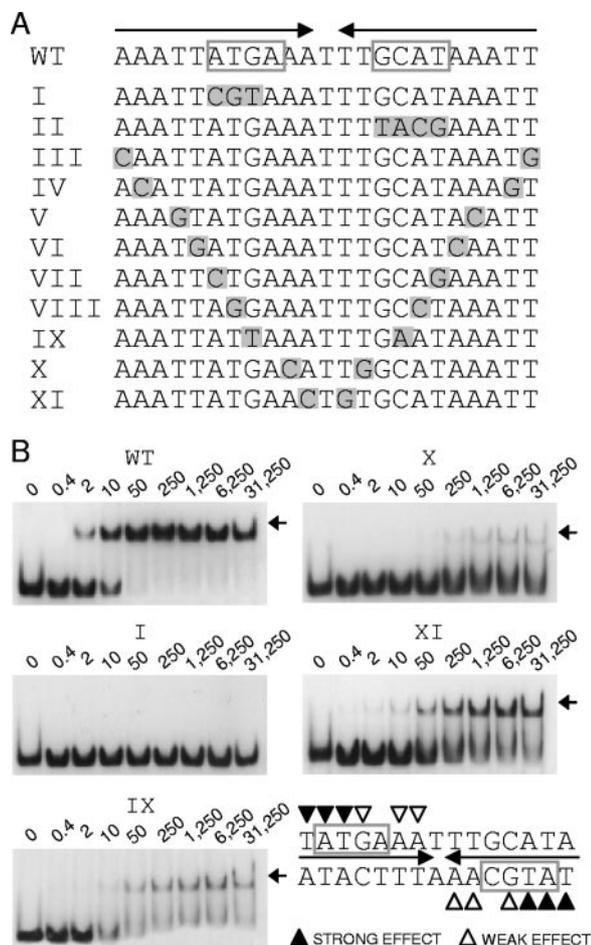
FIG. 5. Characterization of the RsaL^{PAO} DNA-binding site. (A) Sequences of different DNA probes used for EMSA. WT, wild-type probe encompassing the RsaL^{PAO}-binding site on P*lasI*. The repeats forming a palindrome are indicated by arrows. The ATG(C/A) sequences are boxed. Probes I to XI correspond to different mutated variants of the WT probe. Mutated nucleotides are shaded gray. (B) EMSA carried out with RsaL^{PAO} and with the DNA probes indicated above each gel. The concentrations of the different DNA probes were previously equilibrated, and the experiments were carried out simultaneously, with identical polyacrylamide gels run in parallel. The patterns of EMSA carried out with probes III, IV, and V (not shown) were identical to that of probe WT. The patterns of EMSA carried out with probes II, VI, VII, and VIII (not shown) were identical to that of probe I. The RsaL^{PAO}-DNA complexes are indicated by arrows. The protein concentration (nM) for each sample is indicated above its lane. At the lower right is indicated the minimum sequence required for RsaL^{PAO} binding. The triangles indicate the nucleotides whose replacement affects binding.

could not form stable complexes with RsaL^{PAO} (in Fig. 5B, only the EMSA carried out with probe I is shown). Therefore, the specular nucleotides mutagenized in these probes are essential for the formation of the RsaL^{PAO}-DNA complex. Finally, RsaL^{PAO} was able to form unstable, smeared complexes with probes IX to XI, indicating that the specular nucleotides mutagenized in these probes also play roles in RsaL^{PAO} binding. In summary, the above data showed that the palindromic structure of the RsaL^{PAO}-binding site is required for the formation of a stable complex between RsaL^{PAO} and the target

DNA and allowed us to define the minimum half-site for RsaL^{PAO} binding on P*lasI* as TATG(A/C)AA (Fig. 5B).

The RsaL-like proteins. A PSI-BLASTP analysis of the RsaL^{PAO} sequence was performed, retrieving 12 bacterial proteins showing significant levels of homology (Fig. 6) (http://www.ncbi.nlm.nih.gov/BLAST). With the exception of RsaL from *P. putida* strains IsoF, WCS358, and PCL1445 (100% identical), the RsaL homologs are classified as hypothetical proteins. The *rsaL* genes in the above-mentioned *P. putida* strains are located in the intergenic region between *lasR*-like and *lasI*-like genes and have been shown to regulate QS (3, 8, 25). Since acyl-HSL-based QS systems are widespread in bacteria, we asked whether the other *rsaL*-like genes could be involved in QS regulation. Several of the sequenced genomes of bacteria containing RsaL-like proteins contain homologs of the acyl-HSL synthases LasI and/or LuxI (Fig. 6). However, only in the case of *Burkholderia xenovorans* LB400 was the *rsaL*-like gene located in the intergenic region between *lasR* and *lasI* homologs (GenBank accession no. YP_554691 and YP_554693, respectively), suggesting that at least in this strain, the *rsaL*-like gene could behave as a regulator of QS.

DISCUSSION

The regulation of the QS circuitry of *P. aeruginosa* is very complex, since many regulators modulate the production of the QS signal molecules. However, the modes of action of these regulators have been investigated at the molecular level in only a few cases (reviewed in references 22 and 27). To our knowledge, no structural data on any *P. aeruginosa* QS transcriptional regulator have been published. In this study, new insights into the structure and function of the *lasI* transcriptional repressor RsaL^{PAO} are provided.

Since RsaL^{PAO} shows no homology with other DNA-binding proteins, an in silico approach was undertaken to predict the possible tertiary structure of RsaL^{PAO} and its ortholog, RsaL^{WCS}. The model prediction was strengthened by the fact that independent computational procedures selected two structures as templates, λ*c*I-NTD for RsaL^{PAO} and Oct-1 POUs for RsaL^{WCS}, which are identical.

Although RsaL^{PAO} was modeled on the λ*c*I-NTD three-dimensional structure, key functional residues (Arg 20, Gln 38, Ser 42, Arg 43, and Glu 45) are shared with Oct-1 POUs. Both the RsaL^{PAO} and RsaL^{WCS} models show a salt bridge between residues Arg 20 and Glu 45. In Oct-1 POUs, this salt bridge is important for stabilizing the DNA-binding helix, while it is not present in the λ*c*I-NTD three-dimensional structure. Thus, the presence of this salt bridge in the RsaL^{PAO} model was not due to a bias imposed by the choice of the template used to build it. Our analysis confirmed the importance of this salt bridge, since the replacement of either Arg 20 or Glu 45 with Ala abrogated the DNA-binding ability of RsaL^{PAO}, while the reconstruction of the salt bridge in the RsaL$^{R20E-E45R}$ double mutant partially restored DNA-binding ability. RsaL$^{R20E-E45R}$ is capable of a DNA-binding affinity about fivefold lower than that of RsaL^{PAO} (compare the lanes corresponding to 250 nM and 50 nM protein, respectively, in Fig. 3B). This could be explained by considering that in Oct-1 POUs, Glu 45 hydrogen bonds to the conserved Gln 27 residue, in addition to Arg 20 (5). Moreover, the Arg 20 residue of Oct-1 POUs not only

```
▲ Pseudomonas aeruginosa PAO1        ---MASHERTQPQNMAFRA-------------KATRTARRESQETFWSRFGISQSCGSRFENGEN 49
▲ Pseudomonas putida IsoF            ---MKLLNTSAVREVAHQA-------------ISLRLGLKQSQTEFWSRFGISQACASRIECTSQ 49
▲ Nitrosospira multiformis ATCC 25196 -------MKLFEEISNPRE-------------IRRKLGLNQHDFWSKVGVTQSGGSRYESGRN 43
▲ Chromobacterium violaceum ATCC 12472 -------MKLFEKIPNPRE-------------IRRKLGLNQQEFWSRIGVTQSGGSRYESGRN 43
▲ Nitrosomonas europaea ATCC 19718    -------MKLFKSIPNPKE-------------IRQKLGLNQHEFWSKVGVTQSGGSRYESGRE 43
  Neisseria meningitidis Z2491        -------MKIFENIEDVKA-------------IRRKTGLNQIDFWGKVGVTQSGGSRYETGRK 43
  Neisseria gonorrhoeae FA 1090       -------MKIFENIEDVKA-------------IRKKTGMNQIDFWGKVGVTQSGGSRYETGRK 43
  Nitrosomonas eutropha C71           -------MKLFKSIPNPKE-------------IRQKLGLNQQEFWSKVGVTQSGGSRYESGRE 43
▲ Azoarcus sp. EbN1 a                 MPPAKTSNFWFQTNADVVA-------------RRKMLGLNQSEFWMRLGITQSGASRYESGRT 50
▲ Azoarcus sp. EbN1 b                 MPPAKTSNFWFHTNADVVA-------------RRKMLGLNQSEFWMRLGITQSGASRYESGRT 50
▲ Azoarcus sp. EbN1 c                 -------MKNTDTI-DVRE-------------IRRKLGLNQSQFWSKIGVTQSGGSRYESGRN 42
▲ Dechloromonas aromatica RCB         ---MMSTVKTIEKI-DARE-------------IRRKLGLNQQQFWSTLGVTQSGGSRYESGRS 46
▲ Burkholderia xenovorans LB400       ---MELLENHWQPQTGLQARPAEPSTAVDRVLIIAYRKKKKESQRRFWARFGVTQSRGSRFESGAE 63
                                                                         *   .* ** .*::*: .** *

▲ Pseudomonas aeruginosa PAO1         IPFPIYIELHFYIEGQITDRQLADLRGKIRE-------------------------------- 80
▲ Pseudomonas putida IsoF            VPAPVYIELRLYLSGRLEESDLAQ-RPQ----------------------------------- 76
▲ Nitrosospira multiformis ATCC 25196 MPRPVREELVRLVHIEHIDLSKIKKDDLAVAALLKSKDPELYKSLKKASKAKQ----------- 95
▲ Chromobacterium violaceum ATCC 12472 MPKPVREELRLVHVEQIDLSKVRREDFEIVEDLKETHPDLYKSLRKAVRTKIEAQEGGAEAAAS 107
▲ Nitrosomonas europaea ATCC 19718    MPKAVREELRLVHIEHIDLTKIKRDDLIVAAMLKAQYPDLYKNLKKSAKQLK----------- 95
  Neisseria meningitidis Z2491        MPKPVREELRLVHIECIDLAKVNKKDMEIAALLKKHHPDLYAELSKQTKSERKKQS-------- 99
  Neisseria gonorrhoeae FA 1090       MPKPVREELRLVHIECLDLAKVNKKDMEIAALLKKHHPDLYAELSKQTKSERKKQS-------- 99
  Nitrosomonas eutropha C71           MPKAVREELRLVHIEHVDLTRIKRDDLLIAAMLKTQHPDLYKNLKKSAKQLK----------- 95
▲ Azoarcus sp. EbN1 a                 IPNPVKIELQVAYGSDAQMIVTVAELREMPKQPEKQTEKRPQKLIAKKTPRTNDQPRNFGYLP- 113
▲ Azoarcus sp. EbN1 b                 IPNPVKIELQVAYGSDAQTTVAVAELREMPKRPEKQPERR---------------------- 90
▲ Azoarcus sp. EbN1 c                 IPRPVQAELRLVHIEQIDINKVKKEDVEVAEFLKTSNPELYKSLKKEARAKRKERTTR----- 100
▲ Dechloromonas aromatica RCB         MPKPVREELRLVHVEQVDIKSIKRDDWEVVEYLKSQEPELFKSLKKSARSHAKKAA-------- 102
▲ Burkholderia xenovorans LB400       IPAPVREELGLYFTKTVSDADLGRAERVLYSRDAAALLNPGQ------------------- 105
                                       :*  .:  .  *:  .
```
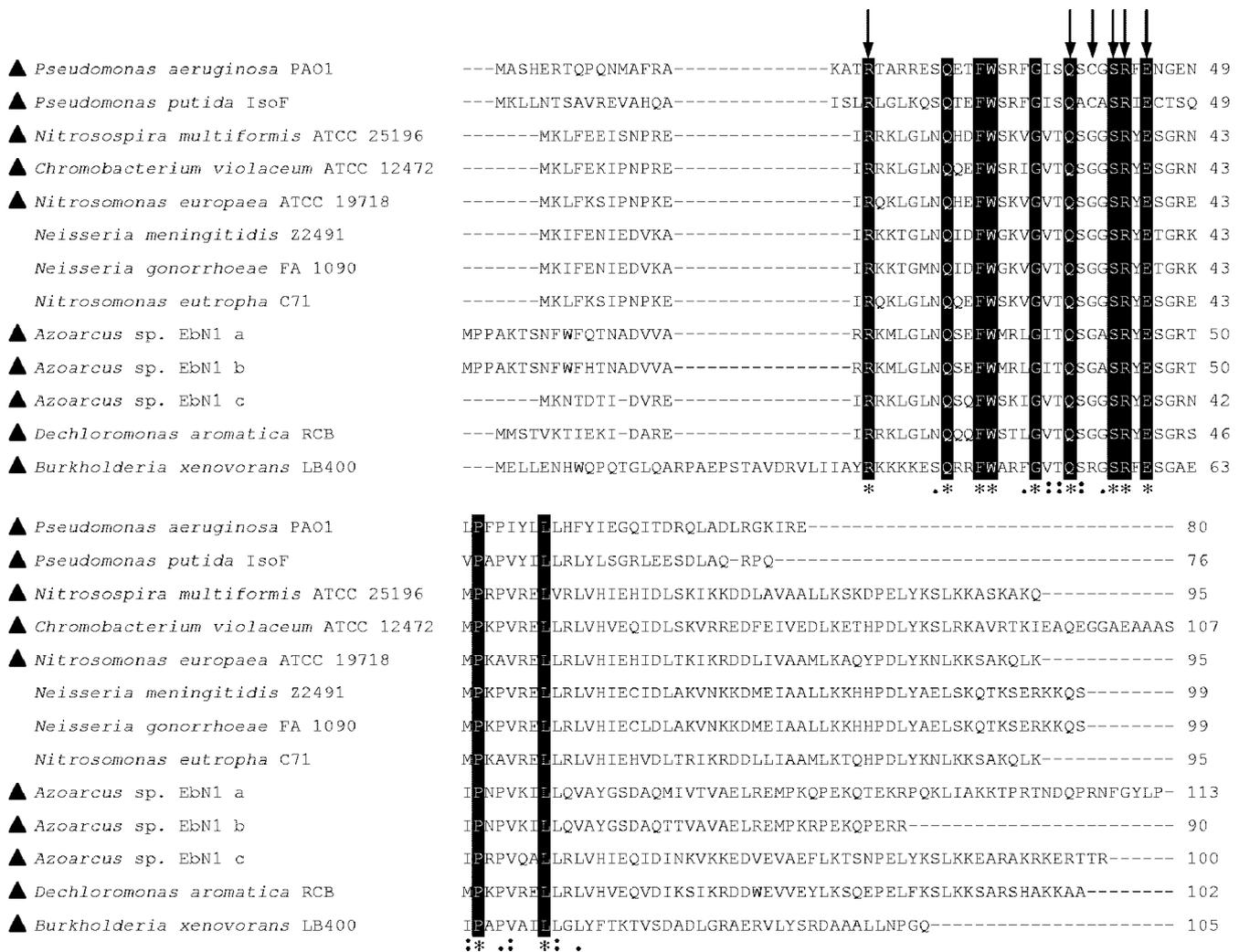
FIG. 6. Alignment of putative bacterial proteins showing significant levels of homology with RsaL^{PAO} in a PSI-BLASTP analysis. The alignment is presented as in the ClustalW ALN output (http://www.ebi.ac.uk/clustalw/) (asterisks, identical residues; colons, conserved substitutions; periods, semiconserved substitutions) with the following modifications: identical residues are also black boxed, residues mutagenized in RsaL^{PAO} are indicated by arrows, and genomes containing *lasI*-like genes are indicated by triangles. GenBank accession numbers are as follows: *Pseudomonas aeruginosa* PAO1, NP_250122; *Pseudomonas putida* IsoF, AAM75412; *Nitrosospira multiformis* ATCC 25196, YP_412629; *Chromobacterium violaceum* ATCC 12472, NP_902047; *Nitrosomonas europaea* ATCC 19718, NP_841560; *Neisseria meningitidis* Z2491, NP_275082; *Neisseria gonorrhoeae* FA 1090, YP_209002; *Nitrosomonas eutropha* C71, ZP_00669043; *Azoarcus* sp. strain EbN1 a, YP_157206; *Azoarcus* sp. strain EbN1 b, YP_195632; *Azoarcus* sp. strain EbN1 c, YP_157355; *Dechloromonas aromatica* RCB, YP_284082; *Burkholderia xenovorans* LB400, YP_554692. Note that the amino acid sequences of RsaL proteins from *P. putida* strains IsoF, WCS358, and PCL1445 are 100% identical.

forms a salt bridge, but also contacts a phosphodiester oxygen of the DNA backbone. It is likely that the same interactions also occur in RsaL^{PAO}, as indicated by the analysis of its structural model. However, the lower in vitro DNA-binding affinity of RsaL$^{R20E-E45R}$ proved to be insignificant in vivo, as shown by the complementation assay.

The residues Gln 38, Ser 42, and Arg 43, which in Oct-1 POUs directly contact an ATGC DNA motif, are also necessary for the DNA-binding activity of RsaL^{PAO}. Our studies of the RsaL^{PAO}-binding site on the *lasI* promoter defined the minimum half-site for RsaL^{PAO} binding on P*lasI* as TATG(A /C)AA. This sequence contains the ATGC motif recognized by Oct-1 POUs and is also similar to the λcI-NTD half-consensus, TATCACCG (11, 12). It is known that the structural similarity between Oct-1 POUs and λcI-NTD corresponds to a striking

similarity in their modes of binding to DNA. Indeed, despite the fact that the amino acids involved in DNA binding are not conserved, these two proteins establish similar networks of interactions with DNA (11, 12). The observation that the DNA sequence recognized by RsaL^{PAO} is also similar to that of Oct-1 POUs and λcI-NTD adds further strength to the structural model proposed for RsaL^{PAO} and indicates that RsaL^{PAO} could dock similarly to DNA. At the quaternary structural level, there are some differences between Oct-1 POUs and λcI-NTD. The latter is a monomer in solution and binds to a pseudopalindromic DNA sequence as a homodimer. In particular, the fifth α helix of λcI-NTD constitutes the dimerization interface (11). Oct-1 POUs do not have a fifth helix and bind DNA as a pseudoheterodimer because they are covalently bound by a flexible linker to a second DNA-binding domain,

the POU homeodomain. Therefore, in Oct-1 POUs the flexible linker functionally replaces the dimerization helix of λcI-NTD (5, 17). In our model, a fifth α helix is also present in RsaL^{PAO}, though it is much shorter than that of λcI-NTD. Our analysis showed that RsaL^{PAO} quaternary organization could be similar to that of λcI-NTD. Indeed, RsaL^{PAO} exists as a monomer in solution but binds to DNA with high cooperativity, as shown by the Hill plot. Moreover a palindromic binding site is necessary for the formation of a stable complex between RsaL^{PAO} and DNA, since disruption of the palindrome leads to lack of complex formation. Due to the high cooperativity, it is very likely that RsaL readily dimerizes in the presence of the palindromic binding site, and thus, intermediate complexes between monomeric RsaL and DNA cannot be detected. It is also possible that the complex between monomeric RsaL and DNA is a low-affinity complex that cannot be detected. Our in vitro results reported here strongly support the notion that the DNA-mediated RsaL^{PAO} dimerization is essential to form a stable DNA-protein complex. This finding is further strengthened by the RsaL^{PAO} dimer modeling (Fig. 5).

As far as RsaL^{WCS} is concerned, in our model, the C-terminal region of the protein is not structured. This could be due to a bias imposed by the template Oct-1 POU structure. However, since the C-terminal region of RsaL^{WCS} is shorter and shares no conserved residues with that of RsaL^{PAO}, the possibility that RsaL^{WCS} binds to DNA as a monomer cannot be excluded.

Proteins containing an H-T-H domain have recently been classified by Aravind and coworkers (1), taking into consideration structural features, the presence of additional domains, and sequence homology. The structural similarity between RsaL, λcI-NTD, and Oct-1 POUs indicates that RsaL belongs to the tetrahelical H-T-H superclass, which constitutes one of the major groups of H-T-H proteins, together with the winged-helix H-T-H proteins (1). On the basis of sequence homology and domain architectures, several distinct protein families have been identified within the tetrahelical H-T-H superclass, including the λcI, AraC, LuxR, LacI, DnaA, TrpR, and TetR families (1). In this analysis, RsaL^{PAO} and three of its homologs (GenBank accession no. NP_902047, NP_275082, and NP_841560) have been considered, but they do not cluster with any of the above-mentioned families (ftp://ftp.ncbi.nih.gov /pub/aravind/HTH/). On this basis, the prokaryotic RsaL-like proteins could constitute a new family of the tetrahelical H-T-H superclass, sharing the following three distinctive features: (i) lack of significant homology with other proteins; (ii) very small size (spanning from 76 to 113 residues), consisting almost exclusively of the four-helix bundle core; and (iii) conservation of key residues. With respect to the last point, the Arg 20, Gln 38, Ser 42, Arg 43, and Glu 45 residues, conserved between RsaL^{PAO}, RsaL^{WCS}, and Oct-1 POUs, are also conserved in the other RsaL^{PAO} homologs, in agreement with our data showing that these residues are important for RsaL^{PAO} function (Fig. 6).

The four-helix bundle is a structure widely present in the three superkingdoms of life (1), suggesting that this fold was probably present in the last universal common ancestor. Given the huge evolutionary distance dividing bacteria and mammals, it is likely that the features shared by RsaL^{PAO} and Oct-1 POUs, and by their cognate promoters, arose by convergent evolution from two distinct regulator-promoter pairs that independently evolved from a common ancestor. However, the possibility that these features have been maintained as ancestral characteristics cannot be ruled out.

REFERENCES

1. **Aravind, L., V. Anantharaman, S. Balaji, M. M. Babu, and L. M. Iyer.** 2005. The many faces of the helix-turn-helix domain: transcription regulation and beyond. FEMS Microbiol. Rev. **29:**231–262.
2. **Assa-Munt, N., R. J. Mortishire-Smith, R. Aurora, W. Herr, and P. E. Wright.** 1993. The solution structure of the Oct-1 POU-specific domain reveals a striking similarity to the bacteriophage l repressor DNA-binding domain. Cell **73:**193–205.
3. **Bertani, I., and V. Venturi.** 2004. Regulation of the *N*-acyl homoserine lactone-dependent quorum-sensing system in rhizosphere *Pseudomonas putida* WCS358 and cross-talk with the stationary-phase RpoS sigma factor and the global regulator GacA. Appl. Environ. Microbiol. **70:**5493–5502.
4. **Bonneau, R., C. Strauss, C. Rohl, D. Chivian, P. Bradley, L. Malmstrom, T. Robertson, and D. Baker.** 2002. De novo prediction of three-dimensional structures for major protein families. J. Mol. Biol. **322:**65–78.
5. **Chasman, D., K. Cepek, P. A. Sharp, and C. O. Pabo.** 1999. Crystal structure of an OCA-B peptide bound to an Oct-1 POU domain/octamer DNA complex: specific recognition of a protein-DNA interface. Genes Dev. **13:**2650–2657.
6. **Corbin, D., G. Ditta, and D. R. Helinski.** 1982. Clustering of nitrogen fixation (*nif*) genes in *Rhizobium meliloti*. J. Bacteriol. **149:**221–228.
7. **de Kievit, T., P. C. Seed, J. Nezezon, L. Passador, and B. H. Iglewski.** 1999. RsaL, a novel repressor of virulence gene expression in *Pseudomonas aeruginosa*. J. Bacteriol. **181:**2175–2184.
8. **Dubern, J. F., B. J. Lugtenberg, and G. V. Bloemberg.** 2006. The *ppuI-rsaL-ppuR* quorum-sensing system regulates biofilm formation of *Pseudomonas putida* PCL1445 by controlling biosynthesis of the cyclic lipopeptides putisolvins I and II. J. Bacteriol. **188:**2898–2906.
9. **Heurlier, K., V. Denervaud, and D. Haas.** 2006. Impact of quorum sensing on fitness of *Pseudomonas aeruginosa*. Int. J. Med. Microbiol. **296:**93–102.
10. **Horton, R. M., H. D. Hunt, S. N. Ho, J. K. Pullen, and L. R. Pease.** 1989. Engineering hybrid genes without the use of restriction enzymes: gene splicing by overlap extension. Gene **77:**61–68.
11. **Jain, D., B. E. Nickels, L. Sun, A. Hochschild, and S. A. Darst.** 2004. Structure of a ternary transcription activation complex. Mol. Cell **12:**45–53.
12. **Klemm, J. D., M. A. Rould, R. Aurora, W. Herr, and C. O. Pabo.** 1994. Crystal structure of the Oct-1 POU domain bound to an octamer site: DNA recognition with tethered DNA-binding modules. Cell **77:**21–32.
13. **Kovach, M. E., P. H. Elzer, D. S. Hill, G. T. Robertson, M. A. Farris, R. M. Roop, and K. M. Peterson.** 1995. Four new derivatives of the broad-host-range cloning vector pBBR1MCS, carrying different antibiotic-resistance cassettes. Gene **166:**175–176.
14. **Lyczac, J. B., C. L. Cannon, and G. B. Pier.** 2000. Establishment of *Pseudomonas aeruginosa* infection: lessons from a versatile opportunist. Microbes Infect. **2:**1051–1060.
15. **Miller, J. H.** 1972. Experiments in molecular genetics, p. 252–255. Cold Spring Harbor Laboratory Press, Cold Spring Harbor, NY.
16. **Miller, M. B., and B. L. Bassler.** 2001. Quorum-sensing in bacteria. Annu. Rev. Microbiol. **55:**165–199.
17. **Phillips, K., and B. Luisi.** 2000. The virtuoso of versatility: POU proteins that flex to fit. J. Mol. Biol. **302:**1023–1039.
18. **Rampioni, G., I. Bertani, E. Zennaro, F. Polticelli, V. Venturi, and L. Leoni.** 2006. The quorum-sensing negative regulator RsaL of *Pseudomonas aeruginosa* binds to the *lasI* promoter. J. Bacteriol. **188:**815–819.
19. **Rasmussen, T. B., and M. Givskov.** 2006. Quorum sensing inhibitors: a bargain of effects. Microbiology **152:**895–904.
20. **Sambrook, J., E. F. Fritsch, and T. Maniatis.** 1989. Molecular cloning: a laboratory manual, 2nd ed. Cold Spring Harbor Laboratory Press, Cold Spring Harbor, NY.
21. **Schuster, M., and E. P. Greenberg.** 2006. A network of networks: quorum-sensing gene regulation in *Pseudomonas aeruginosa*. Int. J. Med. Microbiol. **296:**73–81.
22. **Schuster, M., M. L. Urbanowski, and E. P. Greenberg.** 2004. Promoter

specificity in *Pseudomonas aeruginosa* quorum sensing revealed by DNA binding of purified LasR. Proc. Natl. Acad. Sci. USA **101:**15833–15839.

23. **Seed, P. C., L. Passador, and B. H. Iglewski.** 1995. Activation of the *Pseudomonas aeruginosa lasI* gene By LasR and the *Pseudomonas* autoinducer PAI: an autoinduction regulatory hierarchy. J. Bacteriol. **177:**654–659.

24. **Smith, R. S., and B. H. Iglewski.** 2003. *Pseudomonas aeruginosa* quorum-sensing systems and virulence. Curr. Opin. Microbiol. **6:**56–60.

25. **Steidle, A., M. Allesen-Holm, K. Riedel, G. Berg, M. Givskov, S. Molin, and** L. Eberl. 2002. Identification and characterization of an *N*-acylhomoserine lactone-dependent quorum-sensing system in *Pseudomonas putida* strain IsoF. Appl. Environ. Microbiol. **68:**6371–6382.

26. **Venturi, V.** 2006. Regulation of quorum sensing in *Pseudomonas*. FEMS Microbiol. Rev. **30:**274–291.

27. **Wagner, V. E., J. G. Frelinger, R. K. Barth, and B. H. Iglewski.** 2006. Quorum sensing: dynamic response of *Pseudomonas aeruginosa* to external signals. Trends Microbiol. **14:**55–58.